Influence of nitrogen implantation into the buried oxide on the radiation hardness of silicon-on-insulator wafers*

Tang Hai-Ma(唐海马)[a], Zheng Zhong-Shan(郑中山)[a]†, Zhang En-Xia(张恩霞)[b], Yu Fang(于 芳)[c], Li Ning(李 宁)[c], and Wang Ning-Juan(王宁娟)[c]

[a] *Department of Physics, University of Jinan, Jinan* 250022, *China*

[b] *College of Material Engineering, Shanghai University of Engineering and Science, Shanghai* 201620, *China*

[c] *Institute of Semiconductors, Chinese Academy of Sciences, Beijing* 100083, *China*

(Received 24 January 2010; revised manuscript received 26 April 2010)

In order to improve the total-dose radiation hardness of the buried oxide of separation by implanted oxygen silicon-on-insulator wafers, nitrogen ions were implanted into the buried oxide with a dose of 10^{16} cm^{-2}, and subsequent annealing was performed at 1100 °C. The effect of annealing time on the radiation hardness of the nitrogen implanted wafers has been studied by the high frequency capacitance-voltage technique. The results suggest that the improvement of the radiation hardness of the wafers can be achieved through a shorter time annealing after nitrogen implantation. The nitrogen-implanted sample with the shortest annealing time 0.5 h shows the highest tolerance to total-dose radiation. In particular, for the 1.0 and 1.5 h annealing samples, both total dose responses were unusual. After 300-krad(Si) irradiation, both the shifts of capacitance–voltage curve reached a maximum, respectively, and then decreased with increasing total dose. In addition, the wafers were analysed by the Fourier transform infrared spectroscopy technique, and some useful results have been obtained.

Keywords: silicon-on-insulator wafers, radiation hardness, nitrogen implantation

PACC: 6180E, 7340T, 6170T

1. Introduction

The advantages of silicon on insulator (SOI) technology come from the full dielectric isolation that separates devices from substrate. Compared to bulk silicon complementary metal-oxide-semiconductor (CMOS) integrated circuits (ICs), SOI ICs have a higher speed, lower power and no latch-up effect. Particularly, they have a larger resistance to single event upset and high dose rate transient upset effect.[1,2] However, the buried oxide (BOX) of separation by implanted oxygen (SIMOX) SOI wafers has a large number of hole traps which can capture radiation-induced holes in an ionizing radiation environment. This effect will cause the threshold voltage shift of back gate transistors and the increase of leakage current for SOI devices exposed to ionizing radiation.[3,4] Therefore, the BOX makes hardening SOI devices to total dose irradiation complex. In recent years, hardening the BOX of SOI materials has been widely studied. Barchuk *et al.* fabricated the hardened SOI structure with multi-layer buried dielectric, SiO_2-Si_3N_4-SiO_2, by the zone-melting-recrystallization technique.[5] Yi *et al.* prepared a type of SOI materials by oxygen and nitrogen ions implantation to enhance the radiation tolerance of devices.[6] For SIMOX SOI wafers, Yang, Zhang, Wu and Bi *et al.* researched the hardening method of silicon implantation into BOX.[7–12] Although nitrogen implantation into BOX proved to be another effective method for hardening SIMOX materials, and the impact of nitrogen implantation energy on the radiation tolerance of SIMOX wafers has been discussed in our previous work[13] and by Zhang *et al.*,[14] a systematic and wide research is obviously lacking. The properties of nitrogen implanted wafers should be affected by not only nitrogen implantation energy, but also annealing conditions. However, no effort has been made to study these effects. Thus, this work focuses on the influence of nitrogen implantation into BOX on the radiation hardness of SIMOX SOI wafers, with different post-implantation annealing times, at the same implantation dose and energy. The capacitance–voltage (C–V) technique is used for

*Project supported by the Doctoral Science Foundation of University of Jinan.

†Corresponding author. E-mail: zszheng513@163.com

© 2010 Chinese Physical Society and IOP Publishing Ltd

the characterization of radiation damage of the tested samples. The preliminary optimized annealing time at the specific annealing temperature is obtained for the improvement of radiation hardness of the wafers, and the mechanism is discussed. In addition, the Fourier transform infrared (FTIR) spectroscopy technique is used to analyse the effect of the annealing time on the implantation damage.

2. Experiments and *C–V* characterization

Commercial SIMOX SOI wafers were adopted in this work. The wafer has a 150-nm BOX, 190-nm ⟨100⟩ p-type top silicon layer, and about 500-micron silicon substrate. The resistivities of the top silicon and substrate silicon are between 10–20 Ω·cm. First, nitrogen ions were implanted into the five wafers denoted as D1–D5, respectively, at the same energy with the same dose. Considering the almost identical SOI wafers with those in Ref. [13], an optimized implantation energy 90 keV from Ref. [13] was used for nitrogen implantation. In order to obtain distinguishable results for this work's purpose, the wafers D1–D5 were implanted with a nitrogen dose of 10^{16} cm^{-2}, which is much higher than that in Ref. [13]. During the nitrogen implantation, the wafers were maintained at 300 °C. Then, for the as-implanted wafers D2, D3, D4, D5, the subsequent annealing was performed at 1100 °C in N_2 atmosphere for 0.5, 1.0, 1.5, 2.5 h, respectively. The as-implanted wafer D1 was not annealed, used as an extreme case, so as to clearly observe annealing-induced behaviours. For comparison, a wafer denoted as D0 was not implanted as a control. Finally, for the *C–V* characterization of the wafers, the polysilicon-BOX-semiconductor (PBS) capacitors PBS0–PBS5 were fabricated on D0–D5, respectively. The top silicon layers of D0–D5 were removed firstly by reactive-ion etching. After cleaning and drying, the polysilicon gates of the tested capacitors were made by a standard polysilicon gate process used in CMOS ICs manufacture. An ohmic contact with the silicon substrate was also achieved by preparing a film of polysilicon with the same gate process on the backs, and the structure diagram of a PBS capacitor is shown in Fig. 1(a).

The capacitors, PBS0–PBS5, were irradiated with a Co-60 source at a dose rate of 100 rad(Si)$\cdot$s^{-1}. Before irradiation, the high frequency *C–V* characteristics of all the capacitors were measured by a Keithley 590CV analyser at 1 MHz at room temperature. Then, all the tested capacitors were irradiated with total doses of 1×10^5, 3×10^5, 5×10^5 and 7×10^5 rad(Si). After each of the four irradiations, the high frequency *C–V* measurements were performed at the same conditions as pre-irradiation. Unlike the generally used bias configuration,[13] no gate voltage was applied to the capacitors during irradiation. Thus, the pre- and post-irradiation measured results will reflect the ability differences of radiation-induced carriers to escape from recombination in BOX between the different tested samples under zero electric field. In addition, the wafers were analysed by the FTIR spectroscopy, to understand the changes in BOX's microscopic structure before and after nitrogen implantation and annealing.

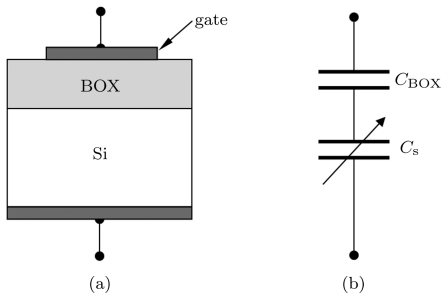


Fig. 1. (a) Cross section of a PBS capacitor and (b) its corresponding equivalent circuit.

According to the *C–V* theory,[15] the interface state capacitance of PBS capacitors is zero at 1 MHz. So, the total capacitance C of a PBS capacitor can be expressed by

$$1/C = 1/C_{\rm BOX} + 1/C_{\rm s}, \tag{1}$$

from Fig. 1(b), where $C_{\rm BOX}$ and $C_{\rm s}$ are the BOX capacitance and the space charge capacitance of the silicon substrate, respectively. Hence, the flat-band capacitance $C_{\rm FB}$ of the PBS capacitor can be written as

$$C_{\rm FB} = C_{\rm BOX}C_{\rm sFB}/(C_{\rm BOX} + C_{\rm sFB}), \tag{2}$$

where $C_{\rm sFB}$ is the high frequency flat-band capacitance of the silicon substrate, given by

$$C_{\rm sFB} = S(\varepsilon_0\varepsilon_{\rm s}Nq^2/kT)^{1/2}, \tag{3}$$

where S is the gate area of the PBS capacitor, ε_0 is permittivity in vacuum, $\varepsilon_{\rm s}$ is the relative permittivity

of silicon, N is doping concentration, k is Boltzmann constant, T is the temperature in Kelvin, and q is electronic charge. Moreover, the normalized flat-band capacitance $C'_{\rm FB}$ of PBS capacitors can be expressed by

$$C'_{\rm FB} = C_{\rm FB}/C_{\rm BOX} = 1\Big/\left[1+\frac{\varepsilon_{\rm BOX}}{\varepsilon_{\rm s}d_{\rm BOX}}\left(\frac{kT\varepsilon_0\varepsilon_{\rm s}}{q^2N}\right)^{1/2}\right]. \quad (4)$$

In addition, the high-frequency minimum capacitance $C_{\rm min}$ and maximum capacitance $C_{\rm max}$ of a PBS capacitor satisfy the relationship

$$C_{\rm min}/C_{\rm max} = 1\Big/\left[1+\frac{\varepsilon_{\rm BOX}}{\varepsilon_{\rm s}d_{\rm BOX}}\left(\frac{4\varepsilon_0\varepsilon_{\rm s}kT}{q^2N}\ln\frac{N}{n_{\rm i}}\right)^{1/2}\right], \quad (5)$$

where $\varepsilon_{\rm BOX}$ is the relative permittivity of BOX, $d_{\rm BOX}$ is the thickness of BOX, $n_{\rm i}$ is the intrinsic carrier concentration. The doping concentration N can be determined from Eq. (5), and then, the normalized flat-band capacitance $C'_{\rm FB}$ can be calculated using Eq. (4). With $C'_{\rm FB}$, the flat-band voltage $V_{\rm FB}$ can be obtained from the measured C–V curves. Therefore, the flat-band voltage shift $\Delta V_{\rm FB}$ can be extracted after irradiation.

3. Results and discussion

Figures 2 and 3 show the typical high frequency C–V curves of the capacitors, PBS0, PBS2, PBS5, before and after irradiation, with the symbols $C_{\rm BOX}$ and $V_{\rm FB0}$ denoting the capacitance of the BOX layer and the initial flat band voltage before irradiation, respectively. Compared with the control sample, PBS0, the C–V curves of nitrogen implanted capacitors also display the large negative shift of $V_{\rm FB0}$, ranging between 9 and 11 V, as summarized in Table 1. In order to compare the radiation effect of the different samples easily, the pre- and post-irradiation C–V curves have been made a shift by $-V_{\rm FB0}$. According to the MOS C–V theory, this large negative shift of $V_{\rm FB0}$ means that the nitrogen implantation of 10^{16} cm^{-2} caused the remarkable increase of fixed positive charge intensity in the BOX layer. Indeed, a high fixed positive charge intensity in BOX will result in negative effects, similar to the radiation-induced total dose responses, on SOI wafers and devices. Therefore, nitrogen implantation doses should be less than 10^{16} cm^{-2} here, to avoid a significant increase in BOX's positive charge intensity.[16,17] On the other hand, the negative shift of flat band voltage $V_{\rm FB}$, after irradiation, is due to the accumulation of radiation-induced trapped holes in the BOX layer. Both the fixed positive charges and the trapped holes can induce the lateral spreading of effective gate area of the capacitors, with their high charge densities in the case of the inversion of substrate surface.[18] Therefore, the high frequency C–V curves are warped near their midgap voltages, because of the significant increase of the BOX's positive charges induced by implantation and irradiation, as shown in Figs. 2 and 3. In this case, the radiation hardness of the samples was characterized using $V_{\rm FB}$ shift, rather than the general midgap voltage shift for its precise value being not obtained. Compared with the pre-irradiation C–V curves, the post-irradiation C–V curves only shift parallelly along the gate voltage axis from Figs. 2 and 3, without stretch distortion caused by interface trapped charges. So it is feasible to apply $V_{\rm FB}$ shift to the quantitative characterization of radiation damage associated with trapped holes in BOX.

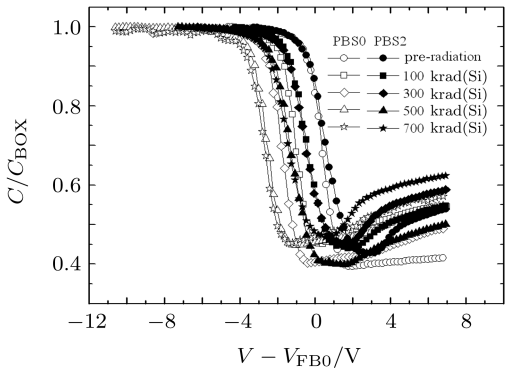


Fig. 2. The pre- and post-irradiation high frequency C–V curves of the capacitors, PBS0, PBS2, with a shift $-V_{\rm FB0}$.

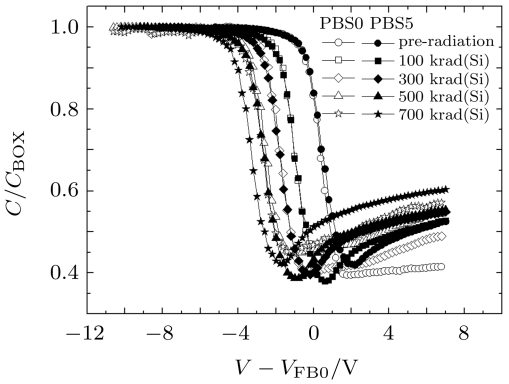


Fig. 3. The pre- and post-irradiation high frequency C–V curves of the capacitors, PBS0, PBS5, with a shift $-V_{\rm FB0}$.

Table 1 illustrates the average value of the negative $V_{\rm FB}$ shifts relative to $V_{\rm FB0}$ for the tested samples after irradiation. It can be found that the radiation hardness of the sample PBS2, with the shortest annealing time after nitrogen implantation, is obviously improved. Compared with the other tested samples, the negative $V_{\rm FB}$ shift of

Table 1. The average values of the $V_{\rm FB}$ shifts of the tested capacitors after irradiation and their $V_{\rm FB0}$s.

capacitors	annealing time/h	pre-rad	100 krad(Si)	300 krad(Si)	500 krad(Si)	700 krad(Si)
		$-V_{\rm FB0}$/V	$-\Delta V_{\rm FB}$/V	$-\Delta V_{\rm FB}$/V	$-\Delta V_{\rm FB}$/V	$-\Delta V_{\rm FB}$/V
PBS0		0.93	1.43	2.46	3.18	3.34
PBS1	0.0	9.38	0.97	2.81	3.04	3.27
PBS2	0.5	11.98	1.16	1.31	2.05	2.23
PBS3	1.0	10.09	1.45	3.27	3.13	2.82
PBS4	1.5	10.38	1.38	4.08	3.58	3.33
PBS5	2.5	9.88	1.44	2.24	3.33	3.88

PBS2 is the smallest after 300, 500, 700 krad(Si) irradiations, respectively, except for that of PBS1 at 100 krad(Si). Therefore, the shorter annealing time should be adopted for hardening SIMOX wafers by nitrogen implantation into BOX. The improvement of radiation hardness is possibly attributed to the two factors, i.e., the release of stress near the interface BOX/Si and the formation of new electron traps in BOX by introduction of nitrogen. In ammonia-nitrided SiO_xN_y gate dielectric, Morokov *et al.* identified that the two-fold coordinated nitrogen atom with an un-paired electron is an electron trap.[19] Also, it is well known that there are strained Si—Si bonds in thermal SiO_2/Si interface, which can become the E' centres with a positive charge by capturing a hole.[20] So, it is reasonable that there should be the same electron traps in nitrogen-implanted BOX as in SiO_xN_y gate dielectric for both having the same composition and structure, and there should also be the strained Si–Si bonds near the BOX/Si interface for the almost same reason. When the strained Si–Si bonds near the interface combine with implanted nitrogen, the release of the interface stress will happen, suppressing the formation of the E' centres, i.e. reducing the number of hole traps associated with the interface stress. On the other hand, the electron traps related to nitrogen will also offset the increase of radiation-induced positive charges in BOX by trapping electrons. As a result, the radiation tolerance will increase. In addition, although the implantation damage was introduced into BOX through nitrogen implantation, it can be eliminated by post-implantation annealing according to the FTIR spectra in Fig. 4. The infrared main absorption band for ion-beam synthesized SiO_2 has been reported at 1050 cm^{-1}, corresponding to Si–O bond.[21] In the present work, except the FTIR spectrum of sample D1 having two absorption peaks at 1098 and 1030 cm^{-1} for implantation damage, the other samples have only a single peak induced by the absorption of Si–O bond at 1090 cm^{-1}, with an increment of 40 cm^{-1} with reference to that in Ref. [21]. This

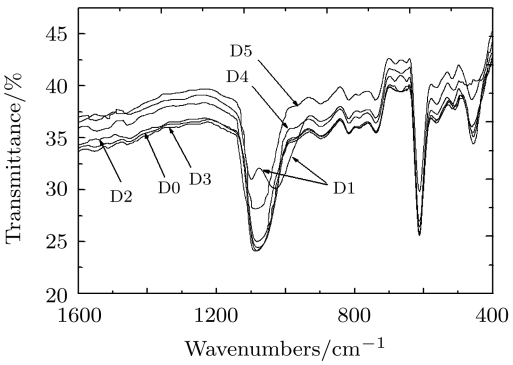


Fig. 4. The Fourier transform infrared (FTIR) spectra of D0–D5 samples. Note that the substrate background corrections in FTIR spectra were done with reference to air.

slight difference between the two peak positions may be due to the different specific processes in preparing materials, leading to a tiny change in BOX microstructure. The point is that the increase of transmittance at 1090 cm^{-1} for sample D1 means the damage of many Si–O bonds, and the FTIR spectrum of sample D2 shows that the elimination of this damage can be basically achieved through a post-implantation annealing for a short time. However, a post-implantation

annealing for a longer time can cause the redistribution of implanted nitrogen ions through the BOX layer, with nitrogen accumulating near the Si/BOX interface on the BOX side.[14] This possibly induces the increase of stress due to too much nitrogen accumulated near the interface, and consequently, more hole traps are formed and the radiation hardness of BOX is decreased, as what PBS3, PBS4 and PBS5 exhibit, compared with PBS2. Moreover, the higher radiation hardness in PBS2 than in PBS0 may be attributed to the release of stress near the interface with nitrogen implantation and the introduction of electron traps associated with implanted nitrogen ions in BOX. As for PBS1, without the post-implantation annealing, its lower radiation hardness than PBS2 is possibly due to hole traps induced by implantation damage. Considering the possible complexity of defects induced by nitrogen ion implantation in BOX, further study on implantation damage is needed for a more detailed explanation.

It also can be found from Table 1 and observed in Figs. 5 and 6 that the total dose responses of PBS3 and PBS4 are different from those of the others with increasing total dose. Both have a maximum $V_{\rm FB}$ shift, respectively, after 300-krad irradiation, and then both $V_{\rm FB}$s begin a reverse shift, i.e. the shift along the positive direction of gate voltage axis, as a result of the increase of irradiation dose, rather than maintaining a negative shift just as the other samples does. So far, the authors of the present paper have not found any reports on this reverse shift. With a lack of further studies on this abnormal shift, it will be difficult to clearly understand its mechanism and give a full explanation for it. In spite of this, seeing that the $V_{\rm FB}$ shifts of PBS3 and PBS4 increase more rapidly and reach their peaks at a lower 300-krad dose of irradiation, this abnormal shift phenomenon maybe indicates that a lot of hole traps in the BOX of D3 and D4 should have much larger capture cross section, and it also suggests that these "large" hole traps occupied by radiation-induced holes, after relaxation, maybe turn to capture electrons for the action of the Coulomb attraction. Namely, an occupied "large" hole trap may tend to become a "large" electron trap, through relaxation induced by capturing a hole. Consequently, the net accumulation of holes will decrease with trapped electrons in BOX for D3 and D4, and the reversed $V_{\rm FB}$ shift happened after subsequent irradiations.

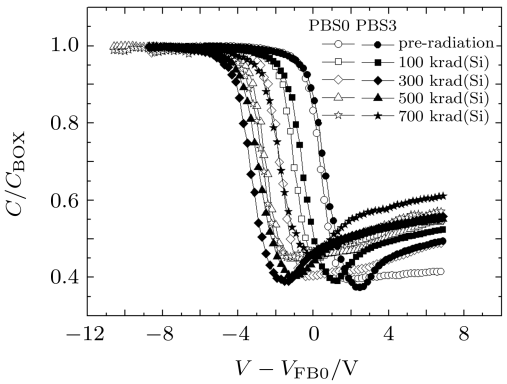


Fig. 5. The pre- and post-irradiation high frequency C–V curves of the capacitors, PBS0 and PBS3, with a shift $-V_{\rm FB0}$.

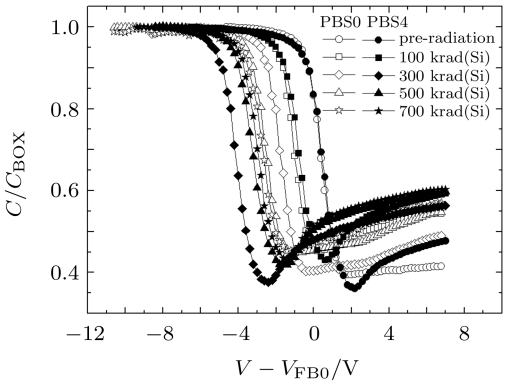


Fig. 6. The pre- and post-irradiation high frequency C–V curves of capacitors, PBS0 and PBS4, with a shift $-V_{\rm FB0}$.

4. Conclusions

Nitrogen ions were implanted into the SIMOX BOX and the post-implantation annealing was carried out for different times to investigate the influence of nitrogen implantation on the total dose radiation hardness of SIMOX materials. The results show that the annealing time can change significantly the radiation responses of the nitrogen-implanted SIMOX materials under different total doses. For a short time of annealing, the material reveals an improved radiation tolerance and the implantation damage can also be eliminated. On the other hand, a long time of annealing caused the decrease of radiation hardness in the case of high total dose radiation. Based on the results, it is also proposed that hole traps with a large capture cross section can become

electron traps. A negative effect of nitrogen implantation into BOX is to introduce positive charges in BOX. Accordingly, nitrogen implantation dose should be restricted to a lower level.

References

[1] Kuo J B and Lin S C 2001 *Low-Voltage SOI CMOS VLSI Devices and Circuits* (New York: Wiley)

[2] Kuo J B and Su K W 1998 *CMOS VLSI Engineering: Silicon-On-Insulator (SOI)* (New York: Kluwer Academic Publishers)

[3] Wolf S 2002 *Silicon Processing for the VLSI Era* (California: Lattice Press)

[4] Schwank J R, Ferlet-Cavrois V, Shaneyfelt M R, Paillet P and Dodd P E 2003 *IEEE Trans. Nucl. Sci.* **50** 522

[5] Barchuk I P, Kilchitskaya V I, Lysenko V S, Nazarov A N, Rudenko T E, Djurenko S V, Rudenko A N, Yurchenko A P, Ballutaud D B and Colinge J P 1997 *IEEE Trans. Nucl. Sci.* **44** 2542

[6] Yi W B, Zhang E X, Chen M, Li N, Zhang G Q, Liu Z L and Wang X 2004 *Semicond. Sci. Technol.* **19** 571

[7] Yang H, Zhang E X and Zhang Z X 2007 *Chin. J. Semicond.* **28** 323

[8] Zhang E X, Sun J Y, Zhang Z X, Qian C, Jiang J, Wang X, En Y F, Luo H W, Shi Q and Zhang X W 2006 *Semicond. Sci. Technol.* **21** 287

[9] Wu A M, Chen J, Zhang E X, Wang X and Zhang Z X 2008 *Semicond. Sci. Technol.* **23** 015015

[10] Zhang S, Zhang Z X, Bi D W, Chen M, Tian H, Yu W J, Wang R and Liu Z L 2009 *J. Semicond.* **30** 093002

[11] Bi D W, Zhang Z X, Zhang S, Chen M, Yu W J, Wang R, Tian H and Liu Z L 2009 *Chin. Phys.* C **33** 866

[12] Zhang E X, Qian C, Zhang Z X, Lin C L, Wang X, Wang Y M, Wang X H, Zhao G R, En Y F, Luo H W and Shi Q 2006 *Chin. Phys.* **15** 792

[13] Zheng Z S, Liu Z L, Zhang G Q, Li N, Li G H, Ma H Z, Zhang E X, Zhang Z X and Wang X 2005 *Semicond. Sci. Tech.* **20** 481

[14] Zhang E X, Sun J Y, Chen J, Zhang Z X and Wang X 2005 *J. Electron. Mater.* **34** L53

[15] Nicollian E H and Brews J R 1982 *MOS (Metal Oxide Semiconductor) Physics and Technology* (New York: Wiley)

[16] Zheng Z S, Zhang E X, Liu Z L, Zhang Z X, Li N and Li G H 2007 *Acta Phys. Sin.* **56** 5446 (in Chinese)

[17] Zheng Z S, Liu Z L, Li N, Li G H and Zhang E X 2010 *J. Semicond.* **31** 026001

[18] Nicollian E H and Goetzberger A 1965 *IEEE Trans. Electron. Dev.* **12** 108

[19] Morokov Yu N, Novikov Yu N, Gritsenko V A and Wong H 1999 *Microelectron. Eng.* **48** 175

[20] Lelis A J, Oldham T R, Boesch H E and Jr McLean F B 1989 *IEEE Trans. Nucl. Sci.* **36** 1808

[21] Gupta G K, Yadav A D, Gundu Rao T K and Dubey S K 2000 *Nucl. Instrum. Method* B **168** 503